Electronic Supplementary Material (ESI) for Journal of Materials Chemistry B.
This journal is © The Royal Society of Chemistry 2018

Electronic Supplementary Information

Crystalline Assembly of Gold Nanoclusters for Mitochondria Targeted Cancer Theranostics

Srestha Basu,[a] Upashi Goswami,[b] Anumita Paul[a] and Arun Chattopadhyay[a,b*]*

[a]Department of Chemistry ,[b]Centre for Nanotechnology, Indian Institute of Technology Guwahati,

Guwahati-781039, Assam, India.

E-mail – arun@iitg.ernet.in, anumita @iitg.ernet.in

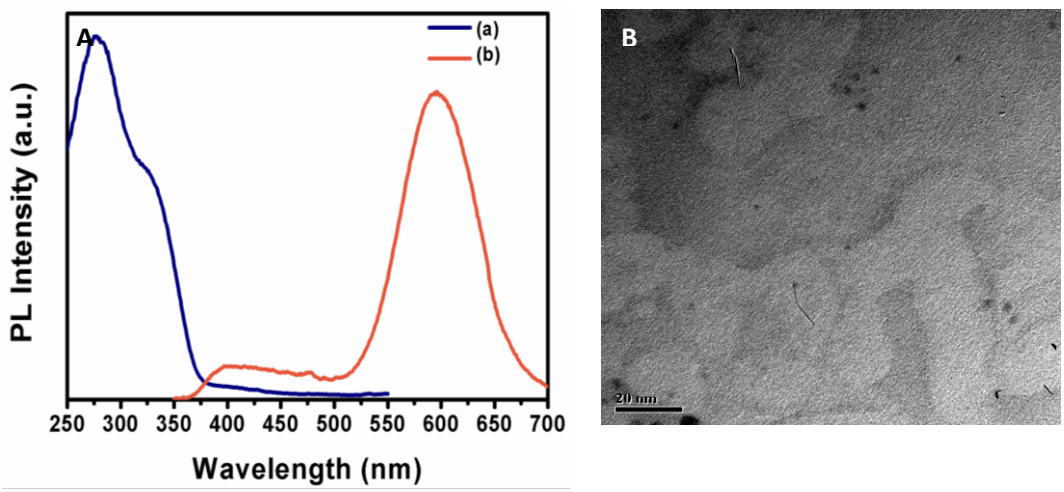

Fig.S1 (A): (a) Excitation and (b) emission spectra of dispersion containing MPA and tyrosine stabilized Au nanoclusters and nanocrystals. (B) Transmission electron microscopic (TEM) image of MPA and tyrosine stabilized Au nanoclusters.

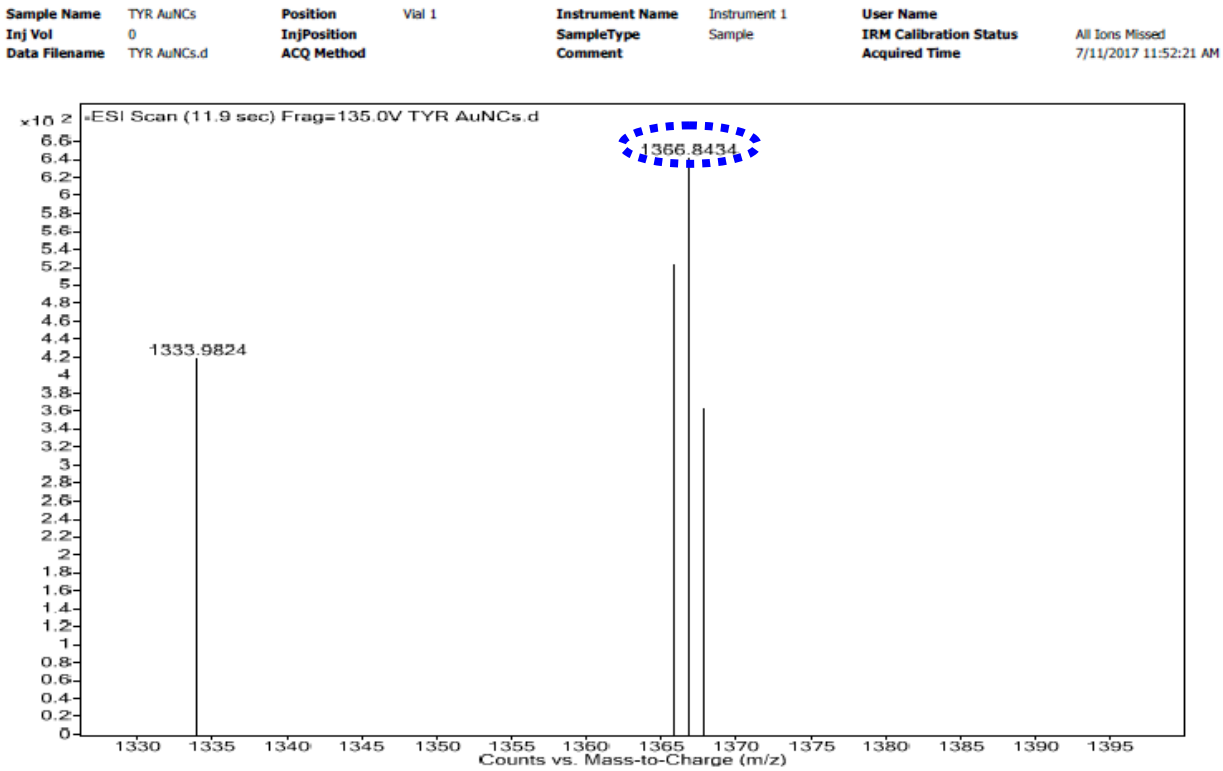

Fig.S2 Electrospray ionization mass spectrometric analysis of MPA and tyrosine stabilized Au nanoclusters. The peak at m/z equal to 1366.84 corresponds to the presence of $[Au_{14}MPA_6Tyr_4 + 3H^+]^{3-}$.

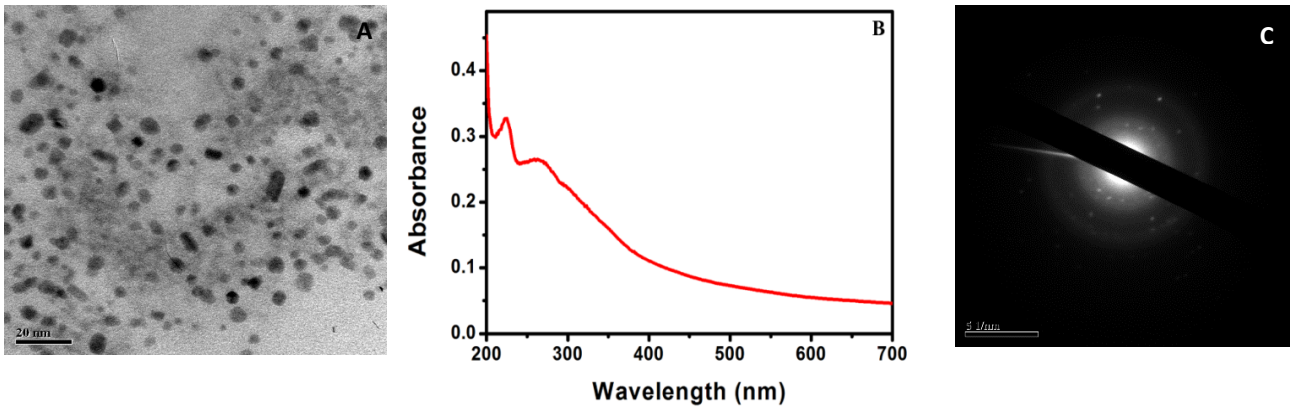

Fig. S3 (A) Transmission electron microscopic (TEM) image and (B) ~~UV-Vis absorbance~~ spectrum of Au nanocrystals formed by association of tyrosine. (C) SAED of a typical particle shown in (A).

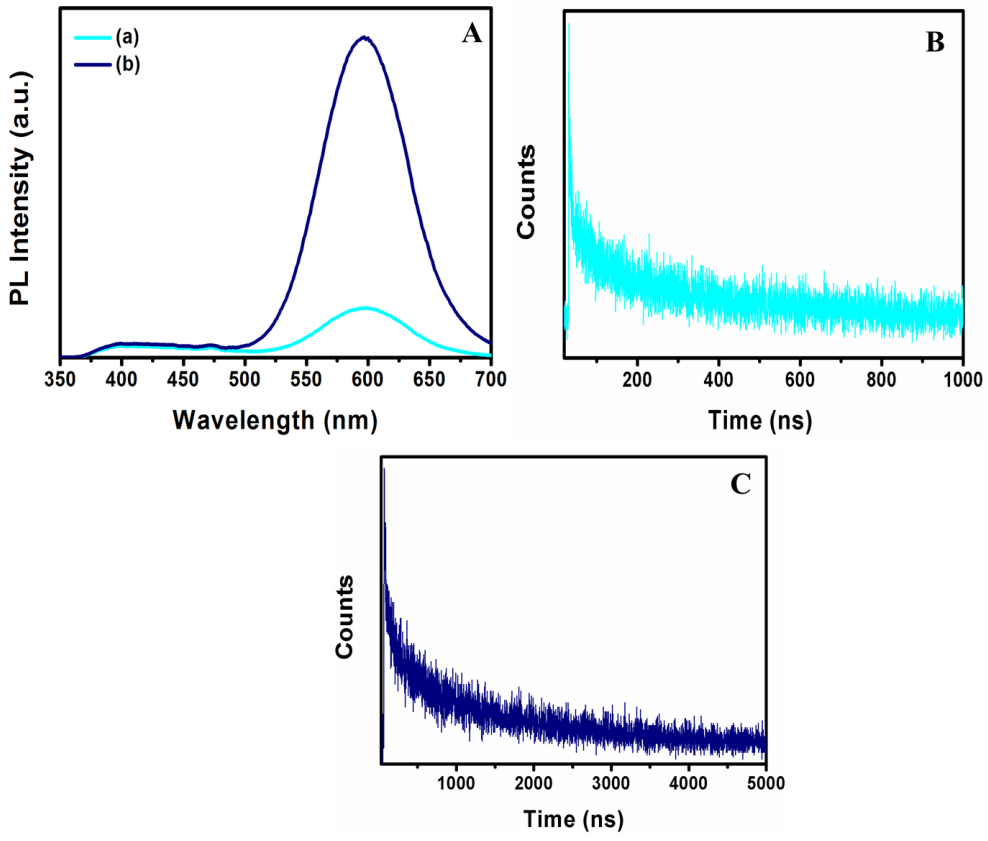

Fig.S4 A) Photoluminescence spectra of (a) Au nanoclusters and (b) product of reaction of Au nanoclusters with zinc ions. Time resolved photoluminescence spectra of (B) Au nanoclusters and (C) the product of reaction between Au nanoclusters and zinc ions.

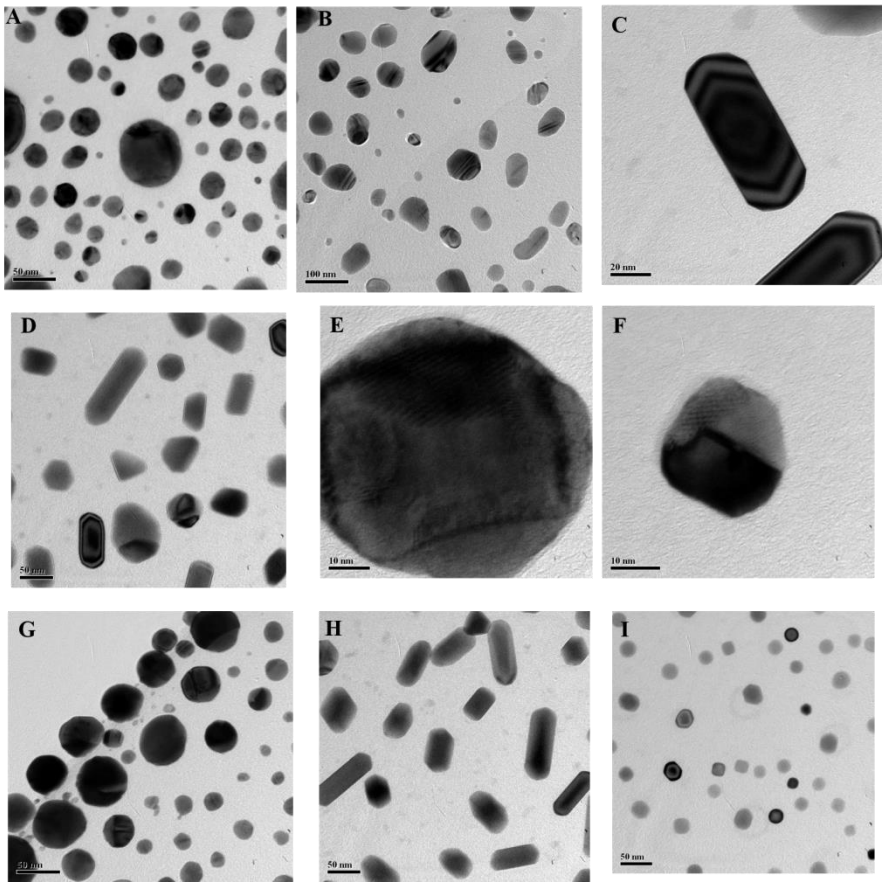

Fig.S5 (A) Additional representative TEM images of the product of reaction between zinc ions and Au nanoclusters (MPA and tyrosine stabilized) performed on different samples as well as recorded on different regions of the same sample.

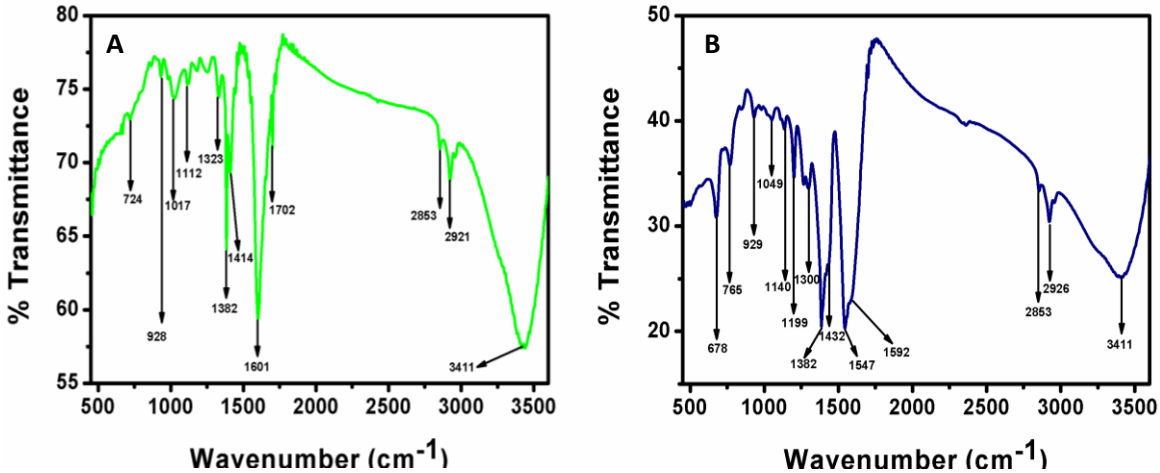

Fig.S6 : FTIR spectra of (A) MPA and tyrosine stabilized Au nanoclusters and (B) the product of reaction between zinc ions and Au nanoclusters.

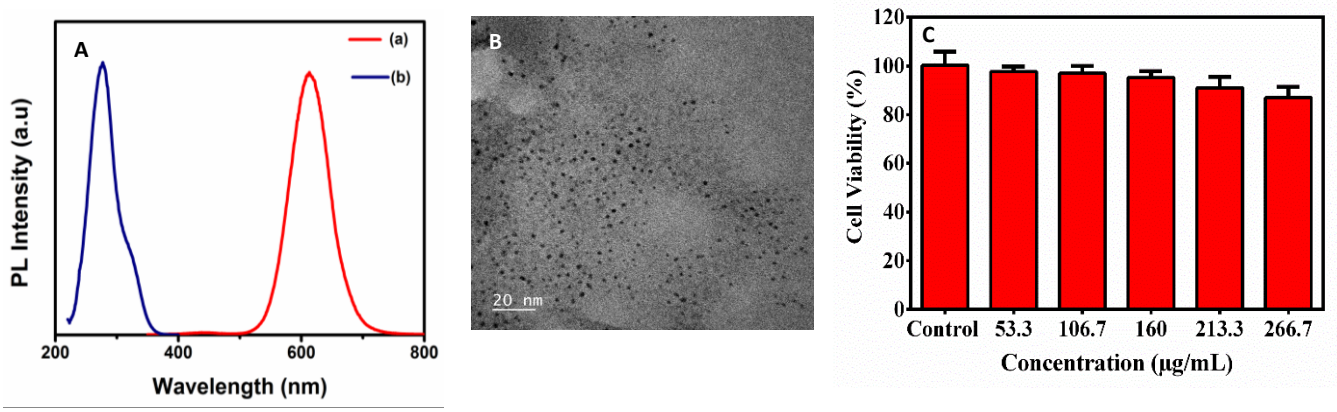

Fig.S7 : (A) (a) Excitation and emission spectrum of mercaptoundecanoic acid stabilized Au nanoclusters (B) TEM image of mercaptoundecanoic acid stabilized Au nanoclusters. (C) MTT assay based cell viability of HeLa cells following treatment with mercaptoundecanoic acid stabilized Au nanoclusters. The results show that ultra-small Au nanoclusters have negligible cytotoxic effect on HeLa cells.

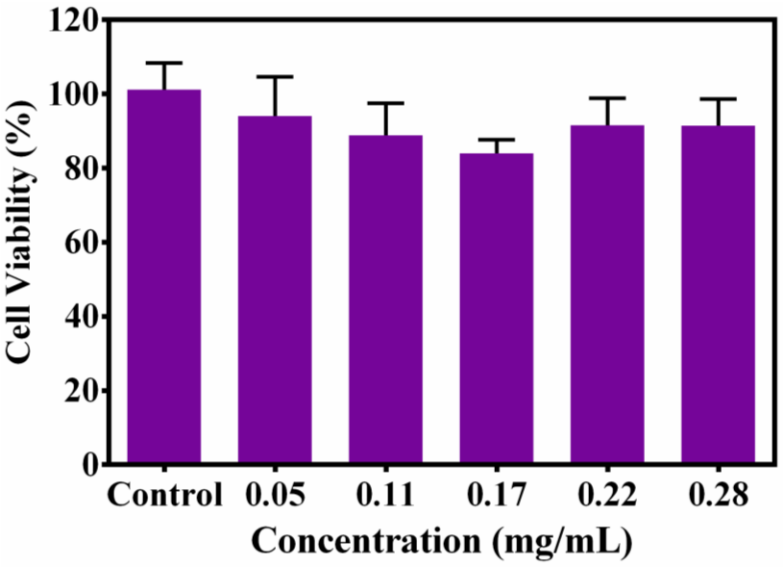

Fig.S8 MTT assay performed on Hela cells following treatment with L tyrosine.

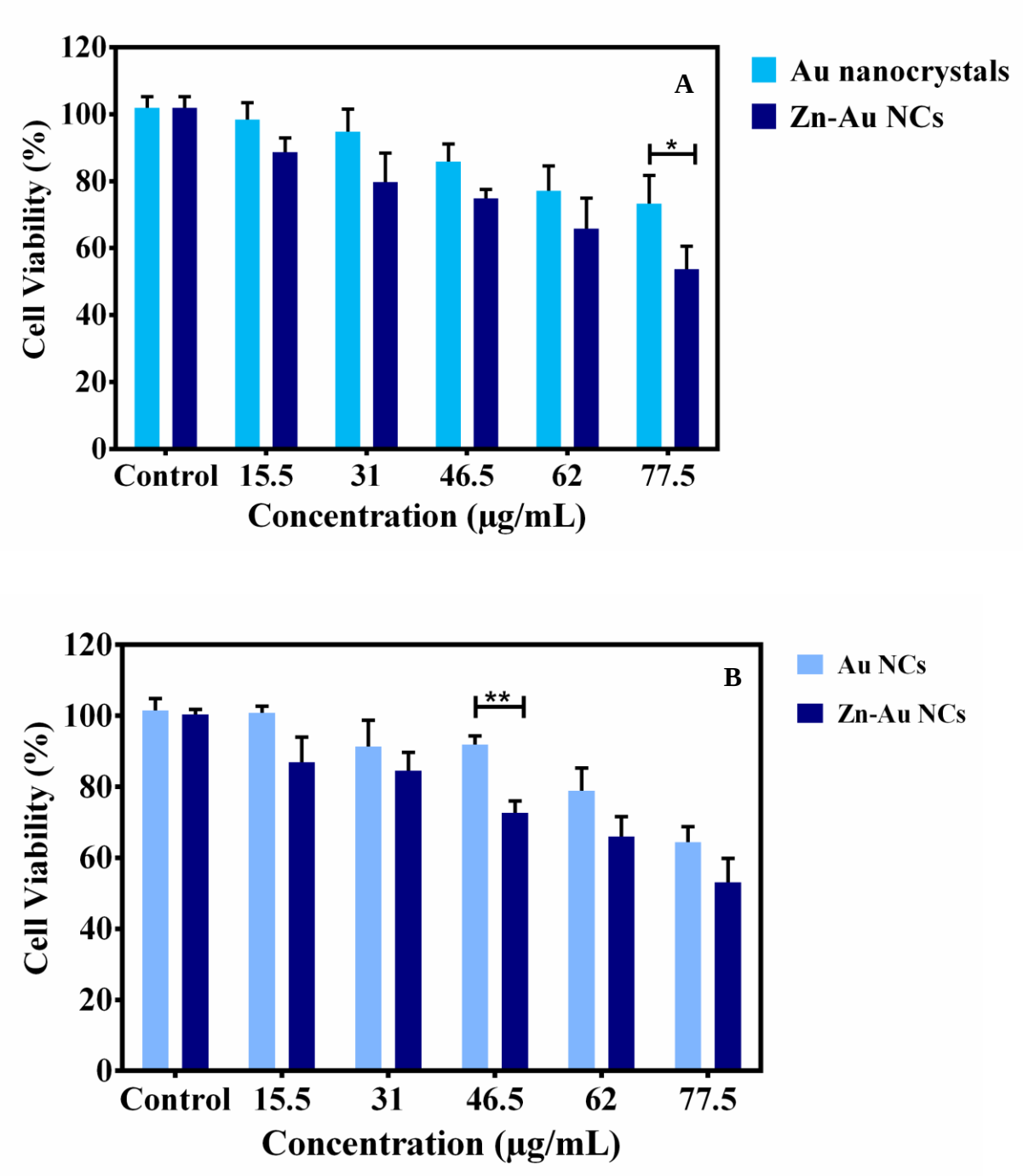

Fig. S9: Representative results of MTT assay based cell viability of HeLa cells upon treatment with Au nanocrystals and Zn Au NCs. These results show that the Au nanocrystals at a concentration of 77.5µg/mL caused ~35% cell death while Zn Au NCs at a concentration of 77.5µg/mL caused ~52 % cell death. These results are shown to support the reproducibility of the results of MTT assay based cell viability of Hela cells upon treatment with Au nanocrystals and Zn Au NCs (shown in Fig. 3 in the manuscript).

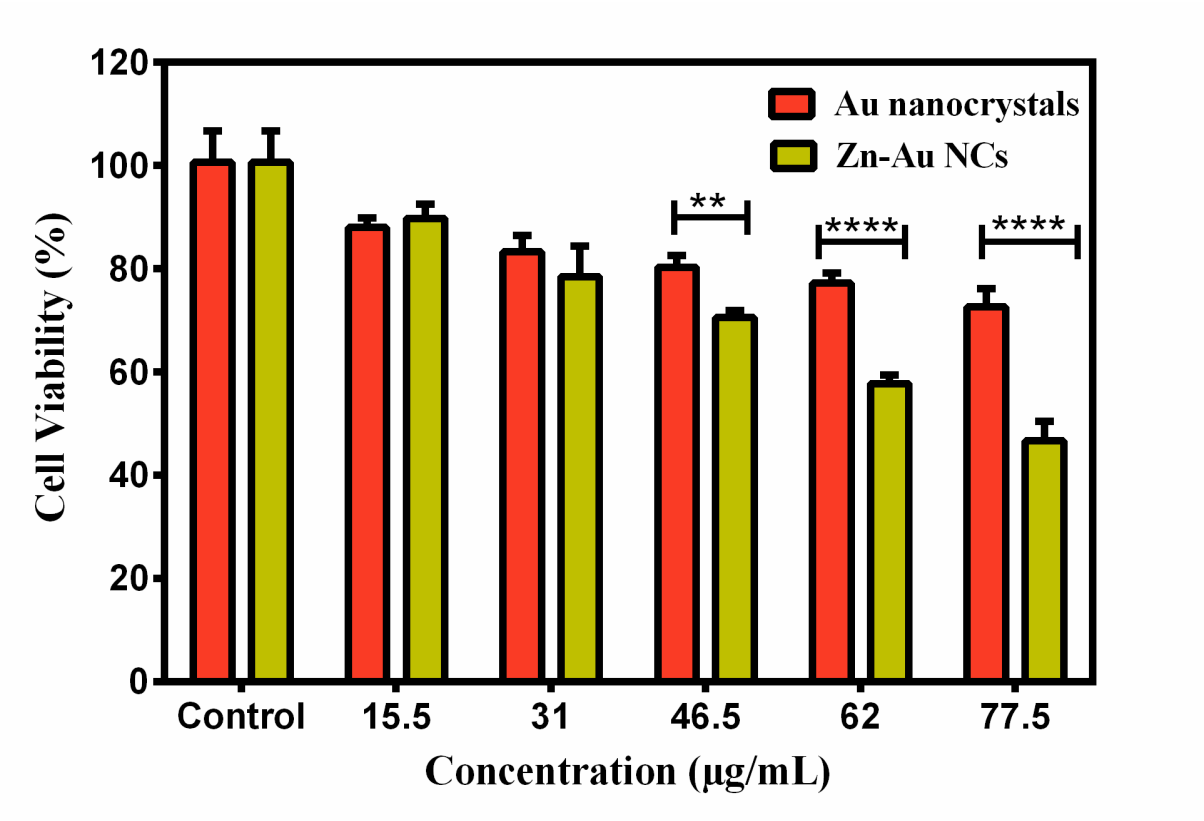

Fig. S10: MTT assay based cell viability of Hela cells treated with dispersion of Au nanocrystals and the Zn Au NCs for 72 h.

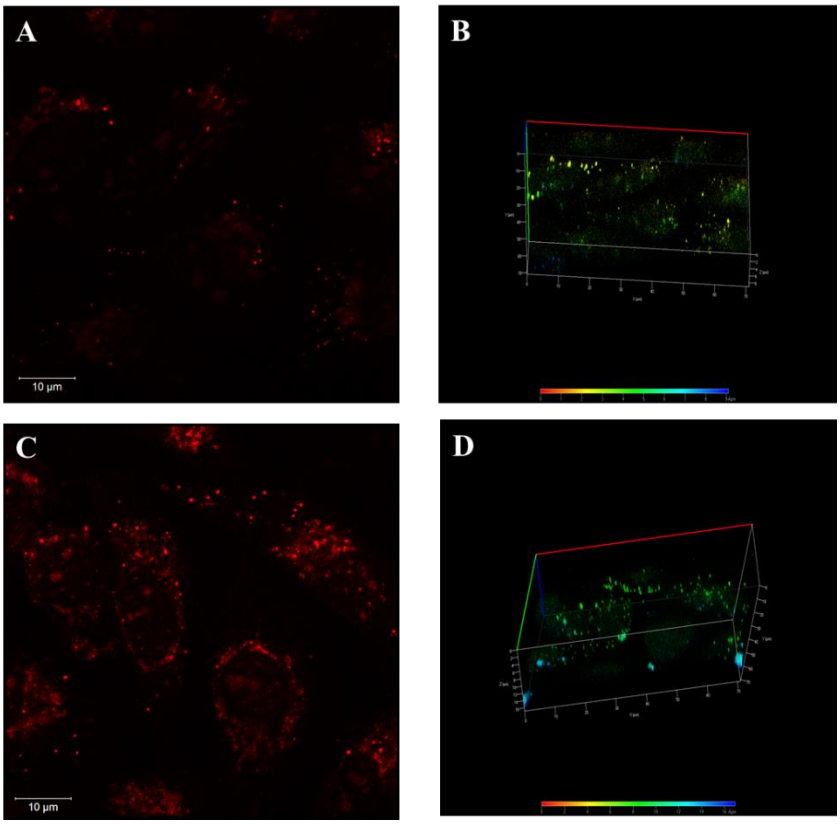

Fig.S11 Confocal laser scanning microscopic analysis of HeLa cells treated with (A) dispersion containing Au nanocrystals and nanoclusters (B) Depth projection analysis of HeLa cells treated with dispersion containing Au nanocrystals and nanoclusters. Confocal laser scanning microscopic analysis of HeLa cells treated with zinc complex of Au nanoclusters and (D) Depth projection analysis of HeLa cells treated with dispersion containing Au nanocrystals and nanoclusters.

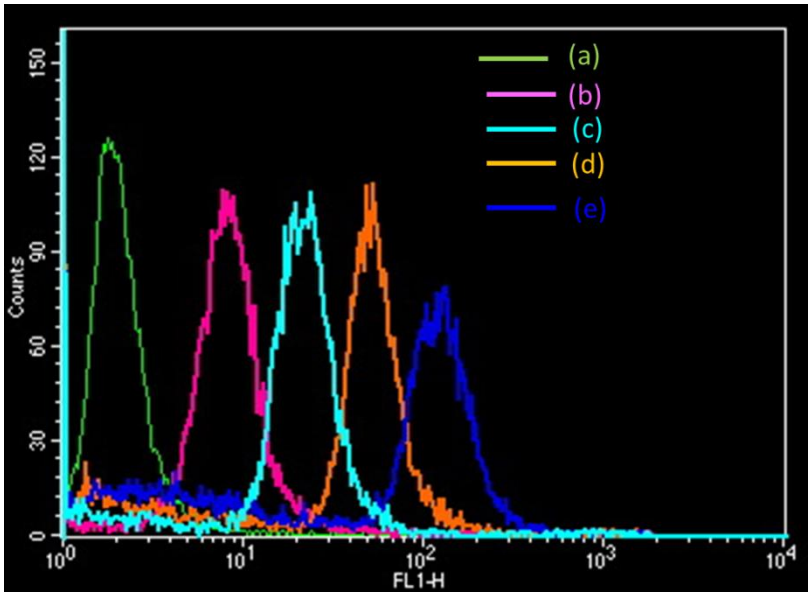

Fig.S12 FACS analysis showing ROS generation. (a) Untreated HeLa cells and HeLa cells treated with (b) 42 µg/mL and (c) 77.5 µg/mL of dispersion containing Au nanoclusters and Au nanocrystals. FACS analysis showing ROS generation of HeLa cells upon treatment with (d) 42 µg/mL and (e) 77.5 µg/mL of zinc complex of Au nanoclusters.

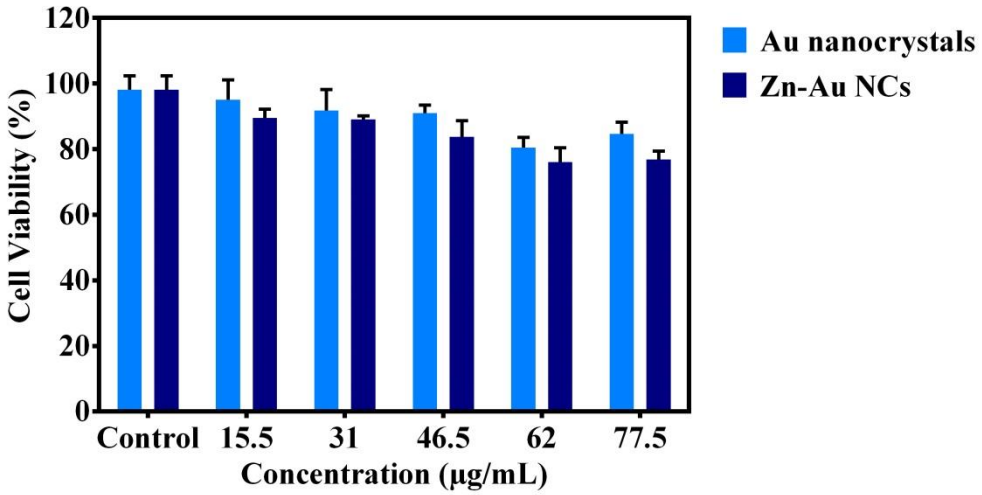

Fig.S13 MTT assay performed on HEK-293 cells following treatment with dispersion of Au nanocrystals and nanoclusters and the product of their reaction with zinc ions.

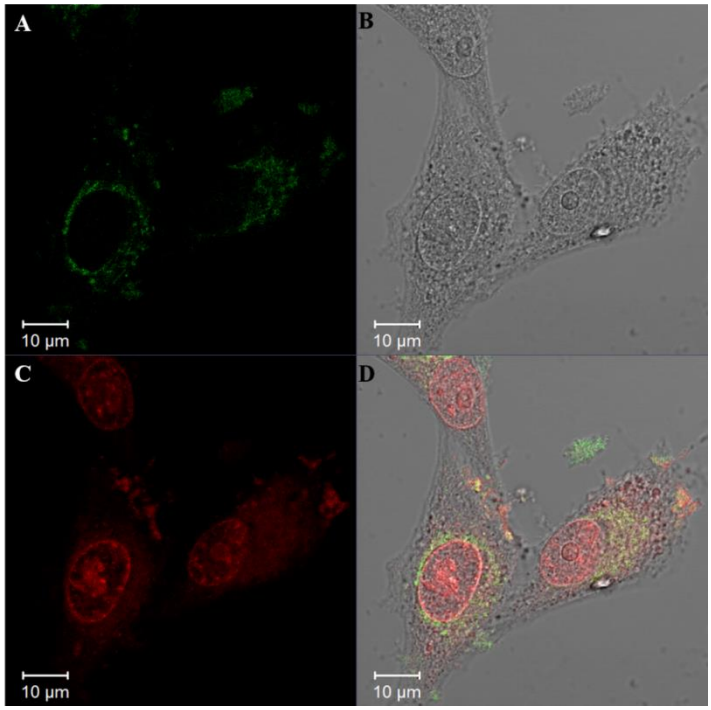

Fig.S14 CLSM images of Hela cells incubated with Au nanoclusters (stabilized with histidine and mercaptopropionic acid) and Mito tracker green acquired in (A) green channel, (B) corresponding bright field image, (C) acquired in red channel, (D) merged images of (A) and (C).

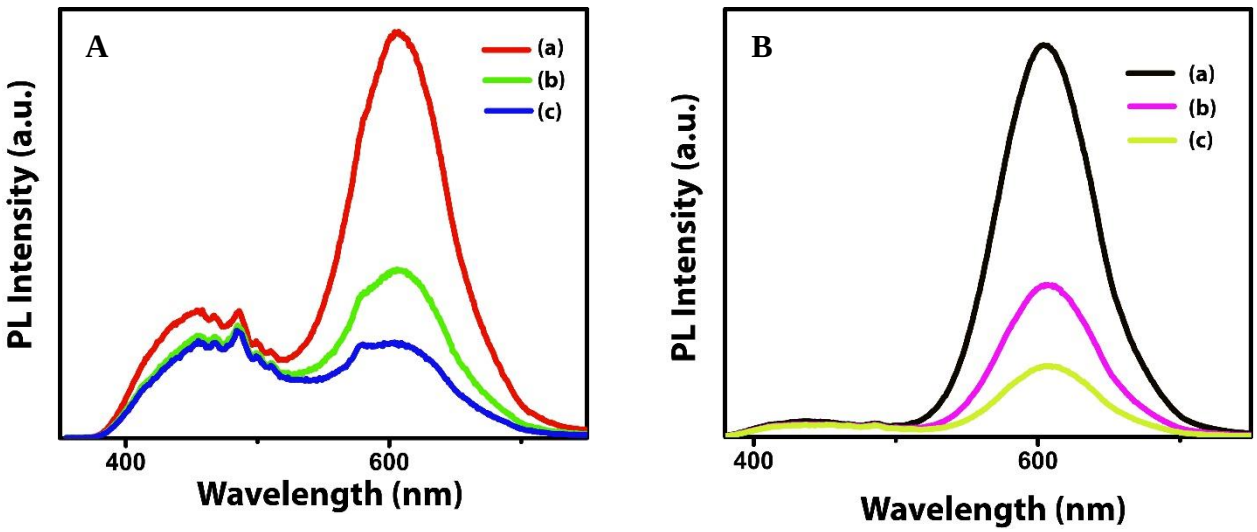

Fig. S15: (A) Luminescence spectrum of (a) Au nanocrystals and that following treatment with (b) 100 µL hydrogen peroxide and (c) 200 µL hydrogen peroxide. **(B)** Luminescence spectrum of (a) Zn Au NCs and that following treatment with (b) 100 µL hydrogen peroxide and (c) 200 µL 37.2 % hydrogen peroxide.

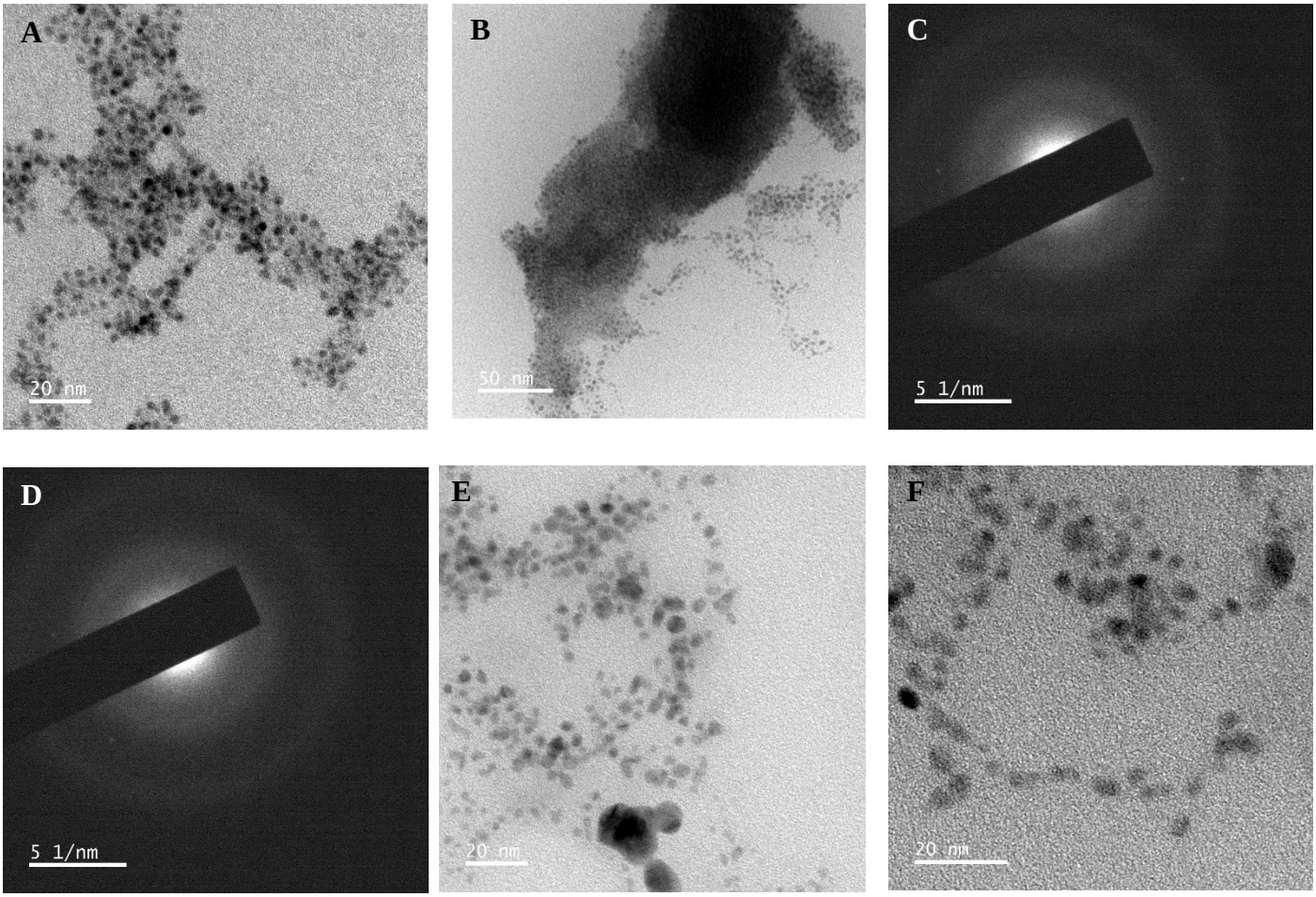

Fig. S16: Transmission electron microscopic (TEM) images of **(A-B)** products of reaction of Au nanocrystals with hydrogen peroxide. These images have been collected in different areas of the TEM grid. **(C-D)** Corresponding selected area electron diffraction (SAED) images. **(E-F)** Additional TEM images of product of reaction of Au nanocrystals with hydrogen peroxide acquired on various areas of the TEM grid.

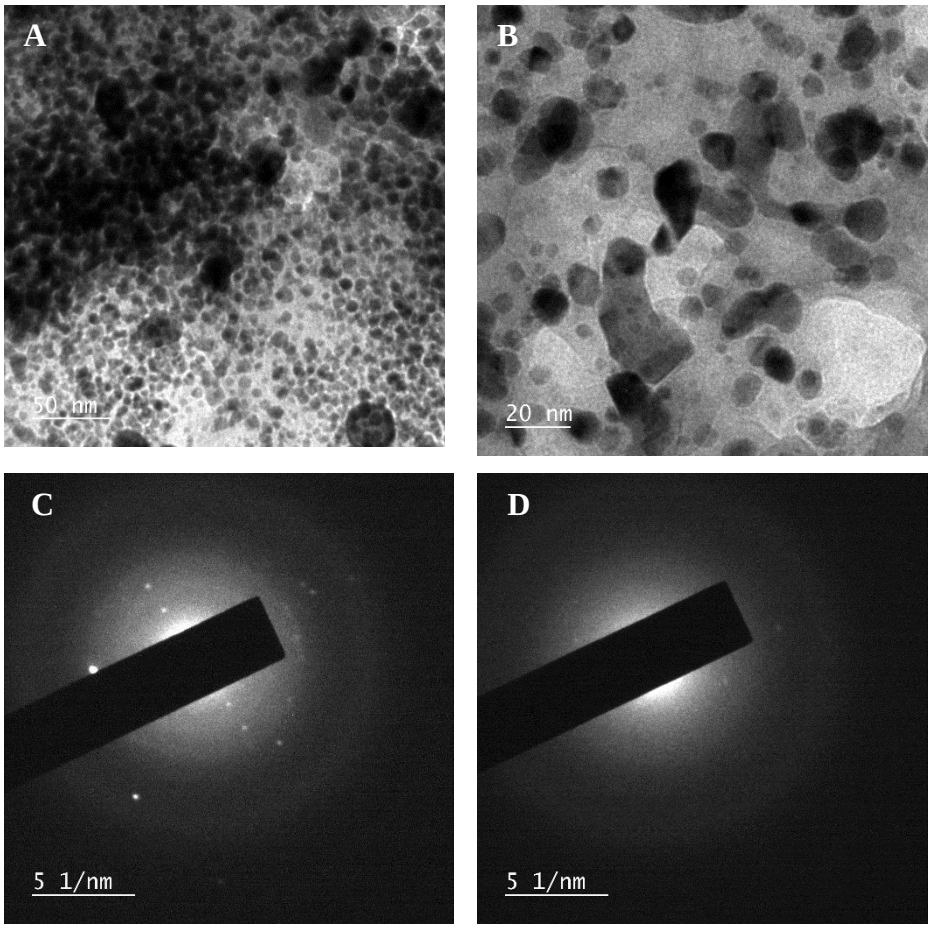

Fig. S17: Transmission electron microscopic (TEM) images of **(A-B)** product of reaction of Zn Au NCs with hydrogen peroxide. These images have been collected in different areas of the TEM grid. **(C-D)** Selected area electron diffraction (SAED) images acquired on typical particles.

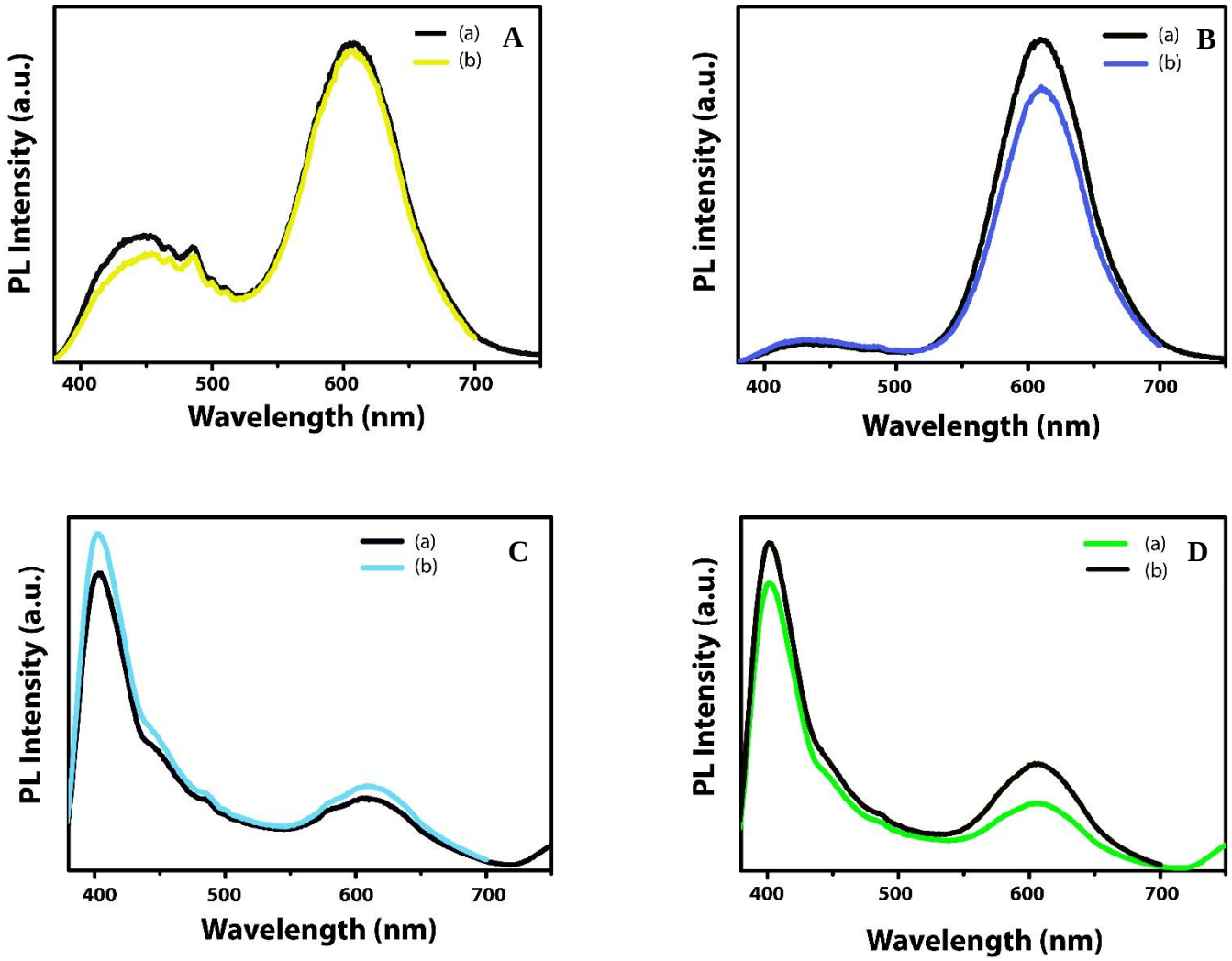

Fig. S18: (A) (a) Luminescence spectrum of Au nanocrystals acquired initially and that (b) after 24 h. **(B)** Luminescence spectrum of Zn Au NCs acquired initially and that (b) after 24 h. **(C)** (a) Luminescence spectrum of Au nanocrystals incubated in human blood serum acquired initially and that (b) after 24 h. **(D)** Luminescence spectrum of Zn Au NCs in human blood serum acquired initially and that (b) after 24 h.

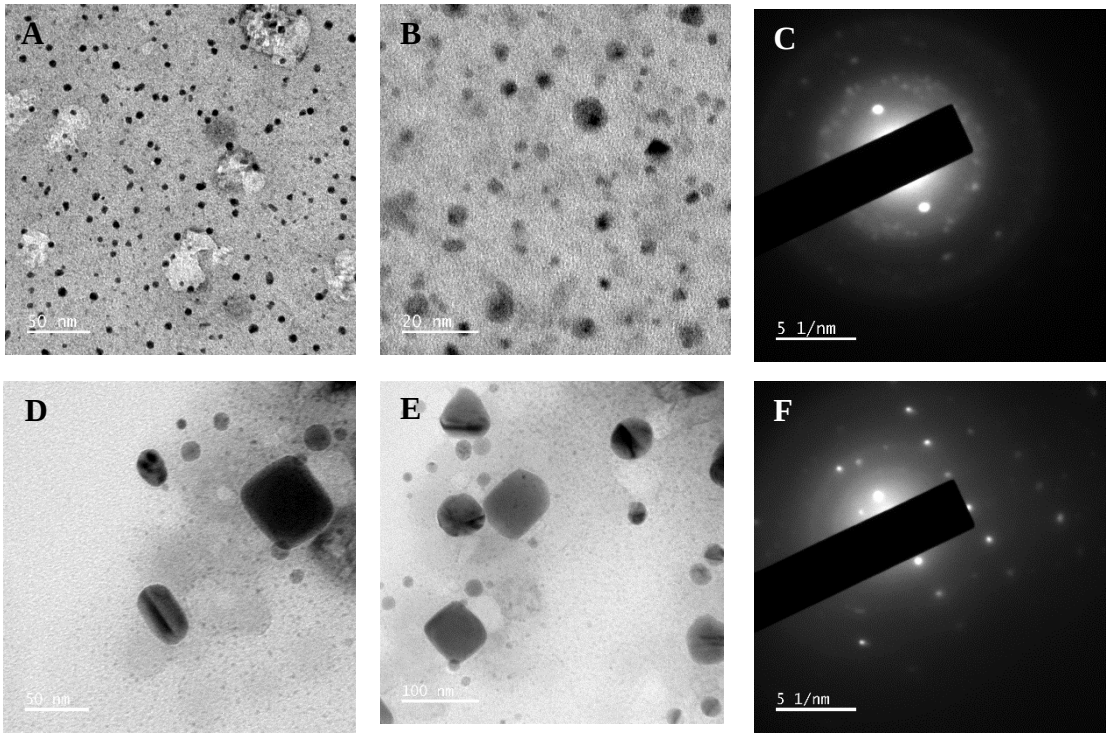

Fig. S19 (A-B): TEM images of Au nanocrystals incubated with human blood serum. **(C)** SAED image acquired for a typical particle. **(D-E)** TEM images of Zn Au NCs incubated with human blood serum. **(F)** SAED image acquired for a typical particle.

Table S1: Time-resolved photoluminescence decay parameters of Au nanoclusters measured prior to and following reaction with zinc ions.

Sample	A1 (%)	τ_1 (ns)	A2 (%)	τ_2 (ns)
Au nanocrystals	9.762	11.661	90.238	255.424
Product of reaction between Au nanoclusters and zinc ions	9.355	105.304	90.645	1453.341

Table S2: A comparative tabulation of percentage cell death of Hela cells upon incubation with Au nanocrystals and Zn Au NCs for 24 h and 72 h.

Sample	Incubation time(h)	Percentage cell death
Au nanocrystals	24	31
	72	28
Zn Au NCs	24	52
	72	54

FTIR analysis:

FTIR spectroscopic analysis was performed to understand the mode of bonding between zinc ions and ligand stabilized Au nanoclusters. The asymmetric stretching frequency due to COO^- of MPA and tyrosine (being attached to the clusters), occurring at 1702 cm^{-1} and 1601 cm^{-1}, were observed to shift to 1592 cm^{-1} and 1547 cm^{-1}, respectively, following complexation with zinc ions. This is attributed to bonding of zinc ions to carboxylate groups of MPA and tyrosine. Additionally, the difference between asymmetric and symmetric stretch of carboxylate group present in tyrosine was measured to be 165 cm^{-1}, which is a typical signature of mono coordinated metal complex. Also, it is worth noting here that the peak due to stretching of –NH group of tyrosine (3411 cm^{-1}) did not undergo significant shift following complexation with zinc ions. This is suggestive of the fact that $–NH_2$ group of tyrosine, which is otherwise involved in stabilization of Au nanoclusters, did not participate in complexation with zinc ions.

Time resolved photoluminescence study:

Luminescence lifetime of ligand stabilized Au nanoclusters was recorded to be 255.42 ns. While following complexation with zinc ions, the luminescence lifetime was measured to be 1.45 µs. As observed, the luminescence lifetime of the clusters increased significantly following complexation with zinc ions. This is primarily attributed to the structural rigidity gained by the ligand-stabilized clusters upon complexation. Au nanoclusters prior to complexation with zinc ions, owing to the structural flexibility, undergo non-radiative decay and hence are associated with low quantum yield and short lived excited state lifetime. However, following association with zinc ions, the clusters gain structural rigidity. This eventually restricts non - radiative decay and instead enhances radiative decay, which accounts for enhanced luminescence quantum yield and excited state lifetime of the clusters upon reaction with zinc ions.

Step-wise formation of Au nanocrystals from Au nanoclusters:

Step 1: ***Formation of Au nanoclusters:***

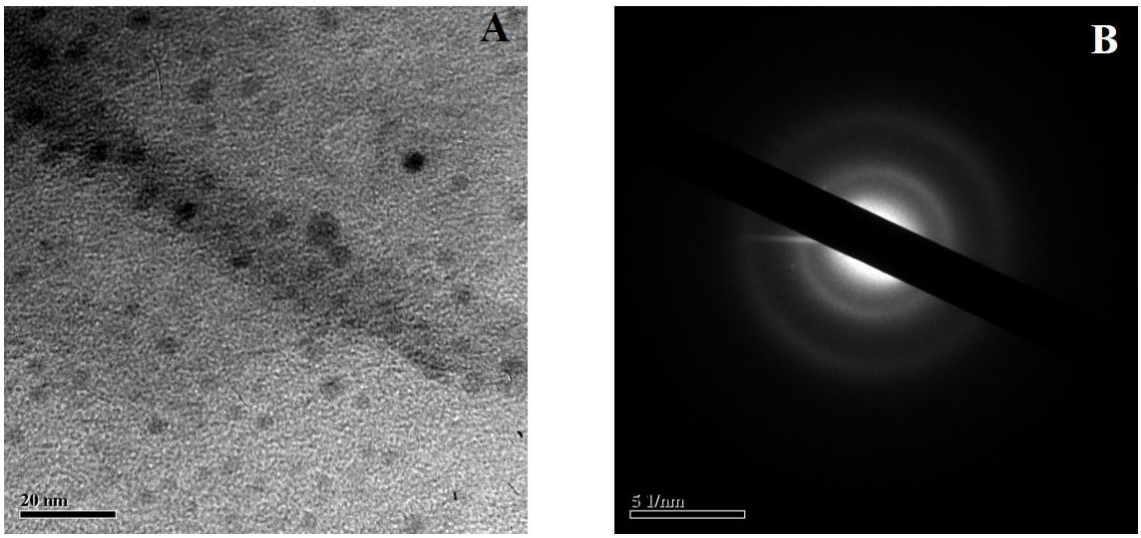

(A) TEM image of MPA and tyrosine stabilized Au nanoclusters (B) Corresponding SAED pattern.

Step 2: ***Growth of Au nanoclusters into Au nanocrystals via ligand association*****.**

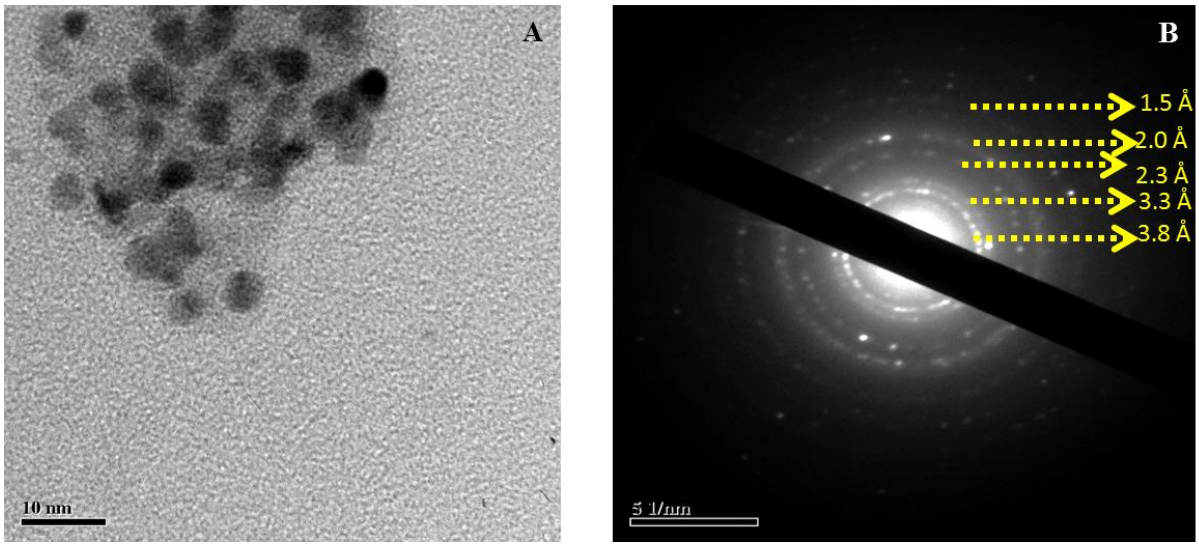

(A) TEM image of Au nanoclusters assembled into nanocrystals via ligand association. (B) Corresponding SAED pattern

Step 3: ***Growth of Au nanoclusters and Au nanocrystals to zinc coordinated nanocrystals.***

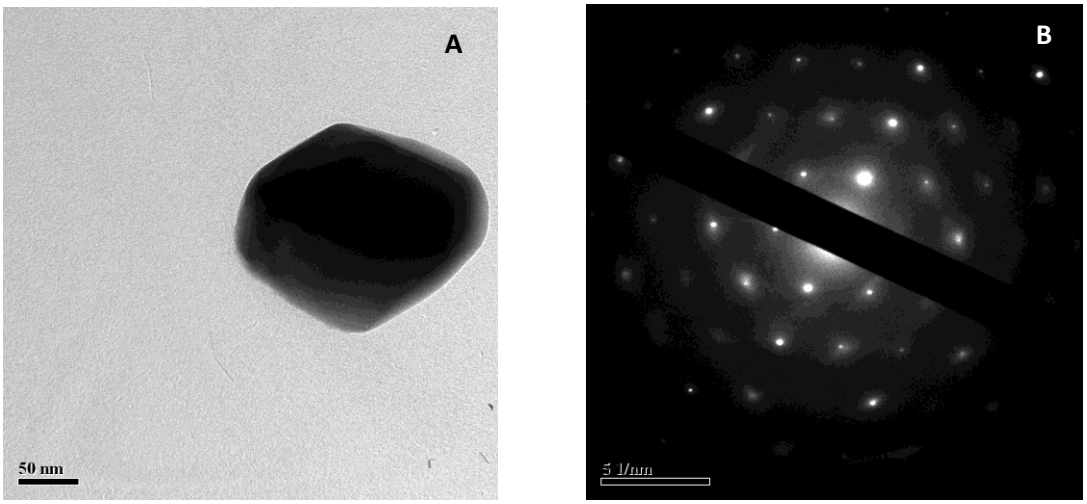

(A) TEM image of zinc coordinated Au nanocrystals. (B) Corresponding SAED pattern.

Plausible mechanism of anticancer activity of assembled Au nanoclusters:

Gold based compounds, owing to their medicinal properties, have been employed as anti-arthritis and anti-inflammatory agents. However, limited anticancer activity of Auranofin - a known anti-rheumatic agent – has expedited the quest for development of gold based anticancer agents. In this regard, substantial amount of efforts has been invested in modification of ligands coordinated to gold (I) to render them as effective anti-cancer agents. However, exploring coordination chemistry on the surface of Au nanoclusters to infuse them with anti-proliferative property would be an interesting approach towards development of newer "nanodrugs". This could, in principle, be achieved via formation of a metal ion mediated crystalline complex (assembly) of Au nanoclusters, where the surface Au atoms are known to be partially oxidized. It would be even better if the constituents of the clusters could specifically interact with the molecules – indispensible for cellular activities - present on the cellular organelles, thereby rendering them inactive and eventually leading to cell death. In this regard, mitochondria, owing to its pivotal role in cell metabolism, have emerged as an important target for cancer therapy. Efforts are being made to design nano vectors to specifically deliver therapeutic molecules to mitochondria. On the other hand, it is known that thioredoxin reductase (TrxR), an enzyme ubiquitous in mitochondria and upregulated in cancer cells, is essential to reduce thioredoxin (Trx). As per literature reports, Au (I) complexes specifically binds to the active site of TrxR. Thus, the enzyme activity of TrxR gets hindered, which finally leads to

mitochondrial damage. Applying this principle to the case of ligand mediated and complexation assisted assembly of Au nanoclusters, targeted killing of cancer cells by specifically causing mitochondrial damage seemed a possibility. This would not only introduce an organelle specific, luminescent anti-cancer nanodrug with therapeutic and diagnostic potential but would also address key issues like drug resistance, limited therapeutic efficacy at ultimate stages of diseases and selective targeting of cancerous cells. Although, deciphering the exact mechanism of action of Zn Au NCs and Au nanocrystals as nanodrugs require much deeper investigations, it may be proposed herein that the activities of Zn Au NCs and Au nanocrystals are due to plausible binding of partially oxidised Au (I) to the active site of TrxR. Since the clusters are stabilized by Tyr and MPA and the active site of TrxR contains thiol containing cysteine, it may be possible that dissociation of Tyr occurs to achieve stronger bonding of gold (I) to thiol group of cysteine. This eventually leads to inhibition of TrxR and thereby affects consequential cellular process, which finally leads to cell death. Further, to highlight the involvement of TrxR in mitochondrial damage, MTT assay was performed on non-cancerous cells (HEK cells) following treatment with nanocrystals and Zn Au NCs and the results were compared to that of Hela cells. TrxR is known to be upregulated in cancer cells in comparison to normal cells. Interestingly, the cytotoxic effect of Au nanocrystals and Zn Au NCs on Hela cells was much pronounced than that on HEK-293 cells (Fig. S12). This could be due to higher expression of TrxR in Hela cells than in HEK cells. A schematic illustration showing the plausible mode of interaction between Au nanocrystals and Zn Au NCs with TrxR is shown below (Scheme 1)[1]

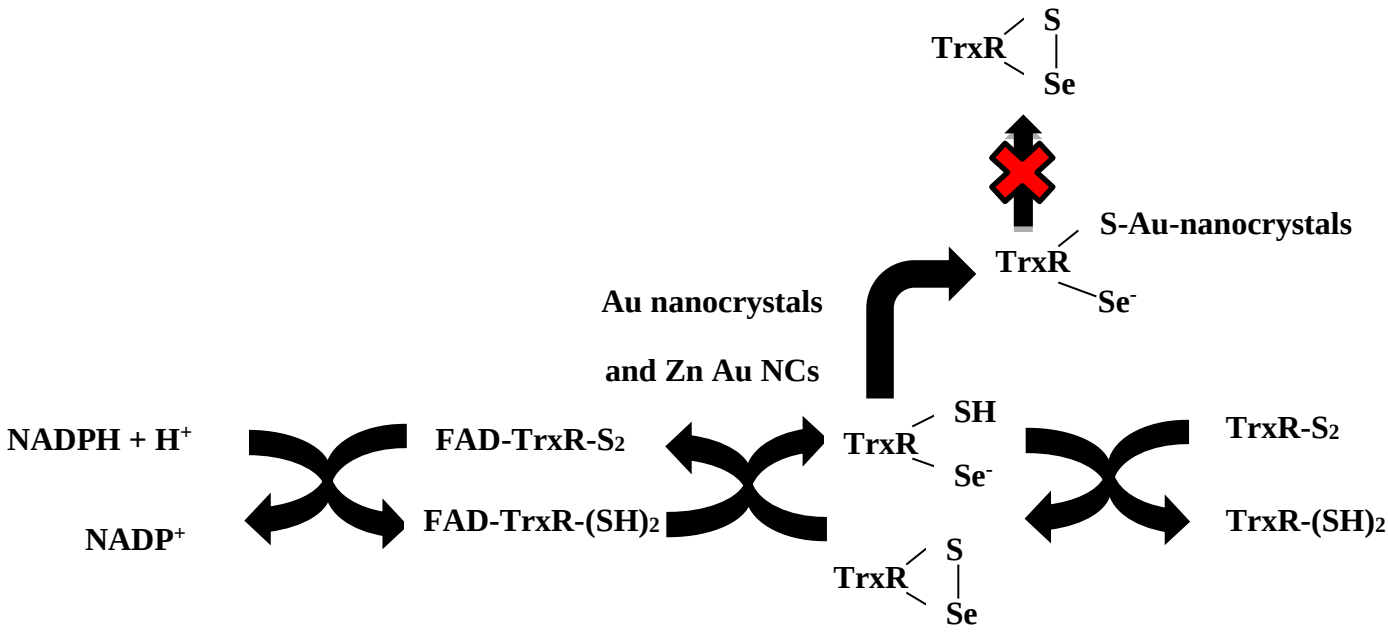

Scheme 1: A schematic illustration showing the plausible mode of interaction between Au nanocrystals and Zn Au NCs with TrxR.[1]

As already stated literature reports suggest the use of Au (I) complexes as mitochondria targeted anticancer agents.[2,3] Several studies have been performed to gain insight into the underlying mechanism of such mitochondria targeted anticancer activity of Au (I) complexes, which revealed preferential binding of Au (I) to thiol groups of thioredoxin reductase (TrxR). This inhibits the enzymatic action of TrxR, leading to consequential mitochondrial damage. A report investigating the detailed mechanism of action of gold complex based inhibitors of TrxR provides crystallographic evidences suggesting the replacement of chloride ion coordinated to gold complex by the thiol group of TrxR.[4] Similarly, in the case of tyrosine (Tyr) mediated assembly of Au nanoclusters, herein referred to as Au nanocrystals, the tyrosine moieties attached to the Au atoms are likely to be replaced by thiol groups (owing to labile nature of the former), which have stronger binding affinity towards Au atoms or Au (I) ions present on the surface of Au nanoclusters. The possibility of such ligand replacement is further supported by a report stating that insufficient thiol ligand stabilized Au nanoclusters may further interact with thiol containing ligands.[5] Another possible mode of interaction between Au (I) (of Au nanocrystals and Zn Au NCs) and TrxR could result from degradation of Au nanocrystals and Zn Au NCs in the presence of ROS. The nanocrystals disintegrated upon interaction with ROS could have exposed Au (I) on their surfaces, which might interact with thiol groups of TrxR.

Explanation for higher cytotoxic activity of Au nanocrystals in comparison to Zn Au NCs:

The extent of cellular uptake and hence the cytotoxic activity of a nanoparticulate drug is crucially determined by the free energy needed for "wrapping" of the same by cell membrane. This is defined by the thermodynamic drive of a particular entity to enter a cell. As per the studies of Warren et al.,[6] the size of a nanoparticle plays critical role in determining the extent to which it would be taken up by a mammalian cell. In an allied study, Gao et al.[7,8] have suggested that nanoparticles in the size range of ~ 55 nm produce sufficient free energy for endocytosis and thus undergo facile cellular uptake following effective wrapping by cell membrane. On the other hand, nanoparticles with size smaller than 50 nm are incapable of producing the amount of free energy required for complete wrapping of the nanoparticles within the surface of the cellular membrane and hence fail to undergo effective endocytosis. Thus, in order to undergo cellular uptake, smaller nanoparticles are clustered onto the surface of the cell to gain the optimum size required to meet the threshold thermodynamic driving force for endocytosis.

In the present study, Au nanocrystals typically were of 5-10 nm. Hence in order to meet the size criterion for endocytosis (~55 nm), Au nanocrystals are to be clustered on the surface of cell membrane. Hence, Au nanocrystals owing to their smaller sizes require an additional interaction among themselves to undergo endocytosis. On the other hand, as synthesised Zn Au NCs with size of ~50 nm need not go through such energy demanding clustering and hence are envisioned to undergo endocytosis in a more facile manner as compared to Au nanocrystals. This may possibly explain the difference between cytotoxic activity of Au nanocrystals and Zn Au NCs.

Plausible mode of internalization of Au nanocrystals and Zn Au NCs in HeLa cells:

A systematic study involving fluorescence based inhibitor assay was performed to delineate the cellular internalization pathway of Au nanocrystals and Zn Au NCs. To this end, there are two

dominant pathways for endocytosis of nanoscale particles – clathrin mediated and caveolae mediated pathways. Our results indicate that caveolae mediated pathway is the primary route for internalization of Au nanocrystals and Zn Au NCs within cell. In order to pursue this, HeLa cells were separately incubated with chlorpromazine (50µM) – a clathrin pathway inhibitor and methyl-β-cyclodextrin (10µM) – a caveolae pathway inhibitor. Thereafter the cells were treated with Au nanocrystals and Zn Au NCs. The uptake of Au nanocrystals and Zn Au NCs was inhibited in presence of clathrin inhibitor by the extent of 30.26% and 21.86%, respectively. On the other hand, the uptake of Au nanocrystals and Zn Au NCs was inhibited by the extent of 53.98% and 62.58%, respectively, in the presence of caveolae pathway inhibitor (Fig. S 20 A-B). This indicated that the uptake of Au nanocrystals and Zn Au NCs occurred primarily through caveolae mediated pathway.

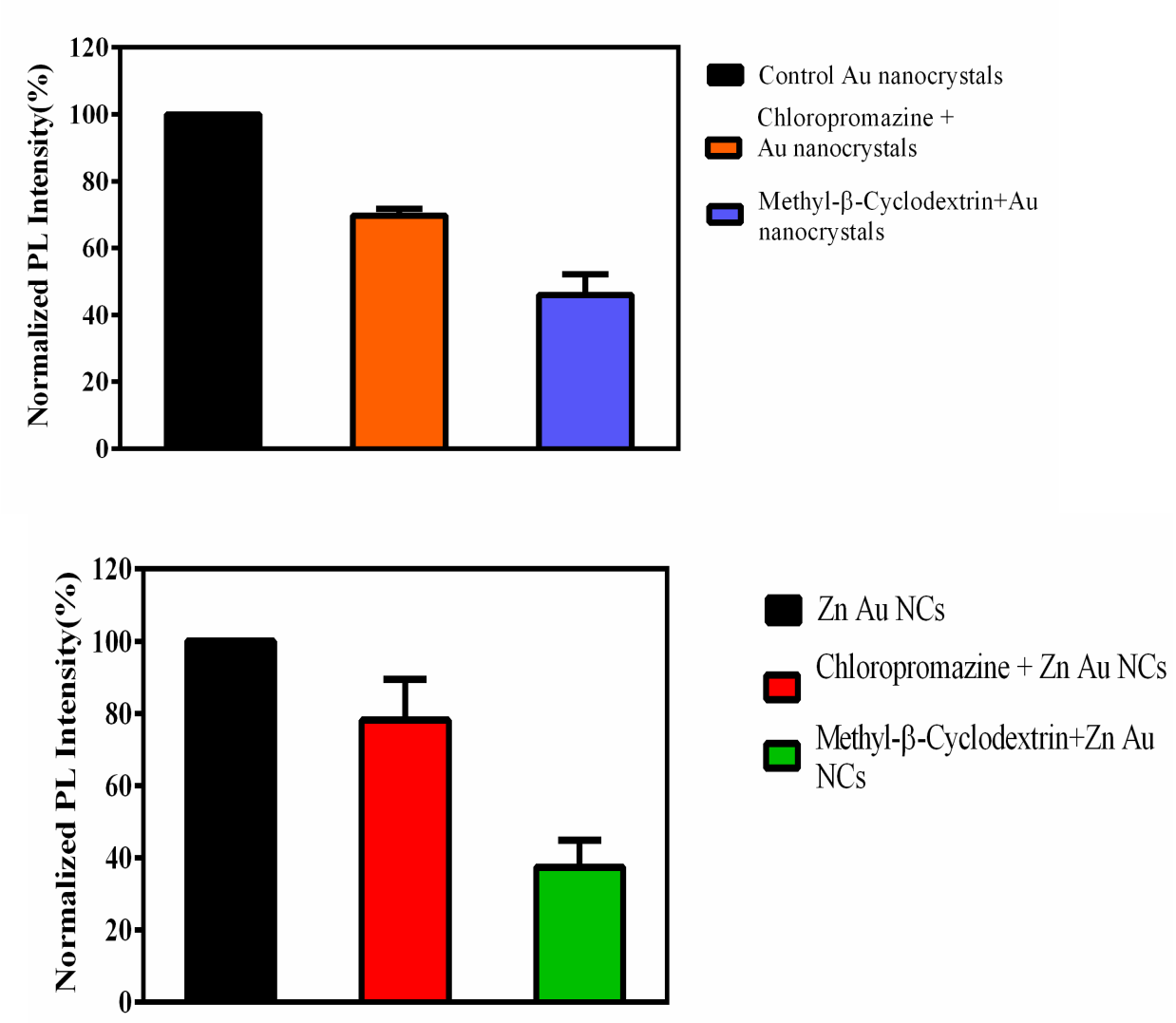

Fig. S 20 A-B: The luminescence intensities of (A) Au nanocrystals and (B) Zn Au NCs following cellular uptake in presence of clathrin and caveolae inhibitor. The reduction in luminescence of Au nanocrystals and Zn Au NCs is indicative of inhibition of their cellular uptake.

Additional figure:

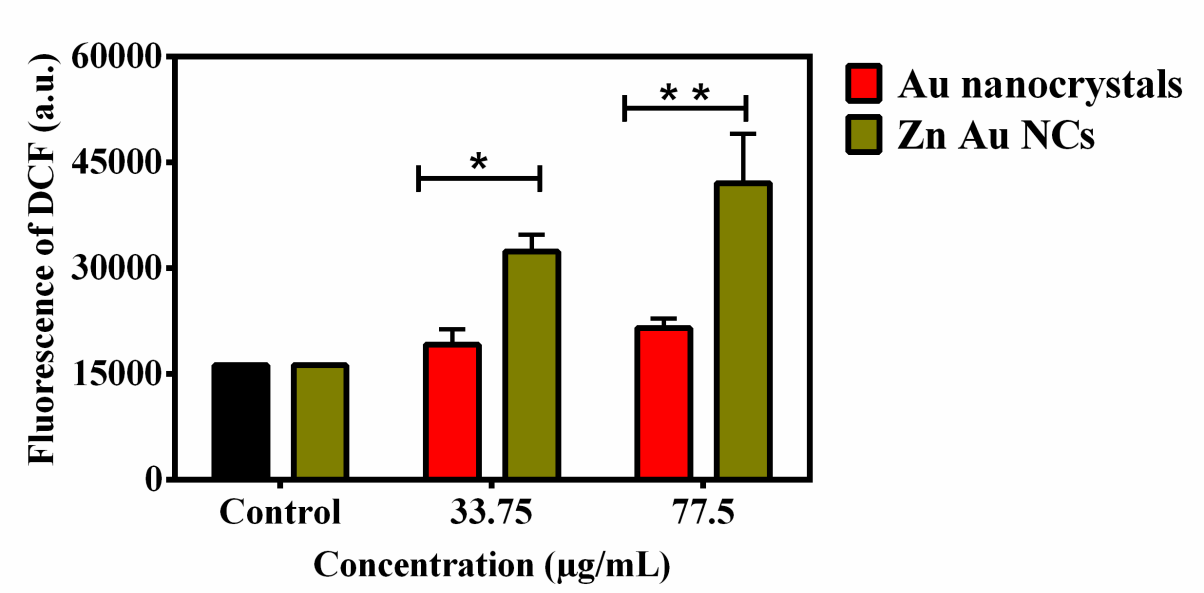

Fig.S21: Quantitative analysis for generation of reactive oxygen species at various concentrations of Au nanocrystals and Zn Au NCs.

References:

1. A. Holmgren and J. Lu, *Biochem. Biophys. Res. Commun.*, 2010, **396**, 120-124.
2. R. Rubbiani, I. Kitanovic, H. Alborzinia, S. Can, A. Kitanovic, L. A. Onambele, M. Stefanopoulou, Y. Geldmacher, W. S. Sheldrick, G. Wolber, A. Prokop, *J. Med. Chem.* 2010, **53,** 8608–8618.
3. G. Ferraro, C. Gabbiani, A. Merlino, *Bioconjugate Chem.* 2016, 27, 1584−1587.
4. S. Urig, K. Fritz-Wolf, R. Réau, C. Herold-Mende, K. Tóth, E. Davioud-Charvet and K. Becker, *Angew. Chem. Int. Ed.*, 2006, **45**, 1881-1886.
5. X. Su, H. Jiang and X. Wang, *Anal. Chem*., 2015, **87**, 10230-10236.
6. B. D. Chithrani and W. C. W. Chan, *Nano Lett.*, 2007, **7**, 1542-1550.
7. H. Gao, W. Shi and L. B. Freund, *Proc Natl Acad Sci U S A*, 2005, **102**, 9469.
8. G. Bao and X. R. Bao, *Proc Natl Acad Sci U S A*, 2005, **102**, 9997.